energies

MDPI

Article

Third-Order Sliding Mode Applied to the Direct Field-Oriented Control of the Asynchronous Generator for Variable-Speed Contra-Rotating Wind Turbine Generation Systems

Habib Benbouhenni [1] and Nicu Bizon [2,3,4,*]

[1] Department of Electrical & Electronics Engineering, Faculty of Engineering and Architecture, Nisantasi University, Istanbul 34481742, Turkey; habib.benbouenni@nisantasi.edu.tr
[2] Doctoral School, Polytechnic University of Bucharest, 313 SplaiulIndependentei, 060042 Bucharest, Romania
[3] Faculty of Electronics, Communication and Computers, University of Pitesti, 110040 Pitesti, Romania
[4] ICSI Energy, National Research and Development Institute for Cryogenic and Isotopic Technologies, 240050 Ramnicu Valcea, Romania
* Correspondence: nicu.bizon@upit.ro

Abstract: Traditional direct field-oriented control (DFOC) techniques with integral-proportional (PI) controllers have undesirable effects on the power quality and performance of variable speed contra-rotating wind power (CRWP) plants based on asynchronous generators (ASGs). In this work, a commanding technique based on the DFOC technique for ASG is presented on variable speed conditions to minimize the output power ripples and the total harmonic distortion (THD) of the grid current. A new DFOC strategy was designed based on third-order sliding mode (TOSM) control to minimize oscillations and the THD value of the current and active power of the ASG; the designed technique decreases the current THD from ASG and does not impose any additional undulations in different parts of ASG. The designed technique is simply implemented on traditional DFOC techniques in variable speed DRWP systems to ameliorate its effectiveness. Also, the results show that by using the designed TOSM controllers, in addition to regulating the active and reactive powers of the ASG-based variable speed CRWP system, the THD current and active power undulations of the traditional inverters can be minimized simultaneously, and the stator current became more like a sinusoidal form.

Keywords: third-order sliding mode control; asynchronous generators; variable speed dual-rotor wind turbine; direct field-oriented control; integral-proportional

Citation: Benbouhenni, H.; Bizon, N. Third-Order Sliding Mode Applied to the Direct Field-Oriented Control of the Asynchronous Generator for Variable-Speed Contra-Rotating Wind Turbine Generation Systems. *Energies* **2021**, *14*, 5877. https://doi.org/10.3390/en14185877

Academic Editors: Surender Reddy Salkuti and Davide Astolfi

Received: 22 August 2021
Accepted: 13 September 2021
Published: 17 September 2021

1. Introduction

A sliding-mode command (SMC) is a robust command technique that forces the system to slide along a prescribed switching surface and changes the dynamics of a system by using a discontinuous command signal [1]. Compared to that of other command strategies, SMC attracted significant interest due to its high robustness to external disturbances, simplicity, ease of implementation, and low sensitivity to the system parameter variations [2]. Similar to other methods, we can find this method in all fields of applied sciences, such as robotics, process command, machine command, and motion command. On the other hand, the instrumentation is among the most widely used applications of the SMC technique. There are new applications of the SMC method, for example, anomaly detection and congestion command. SMC technique was used for AC machine drive in wind turbines. In [3], the author uses the SMC technique to regulate the power of the induction generator. In [4], direct power command (DPC) was designed based on the SMC method of the induction generator. Active power undulations were reduced by using the neural SMC (NSMC) technique [5]. However, the NSMC technique was able to offer better effectiveness and performance compared to that of classical SMC strategy. Benbouhenni et al. proposed the fuzzy SMC technique to reduces stator current and torque undulations of an asynchronous

generators-based wind turbine [6]. This technique combines the advantages of fuzzy logic and the classical SMC technique so the chattering phenomena are eliminated. In [7], a robust SMC technique based on neuro-fuzzy controllers was developed for ASG.

Despite the many advantages and numerical simulation results, as well as the experimental results, the SMC method is still characterized by several problems, such as the chattering issue. When this method is used to produce electricity from a wind farm, it presents ripples at the level of effective electric current, and this is undesirable because high-quality current and energy can be obtained only if the ripple ratio is very small. There are several solutions proposed to ameliorate the characteristics and effectiveness of the SMC technique, and thus, to improve the quality of the electric current. When the current is high quality, the life of the devices is extended to a longer period, thus reducing the cost of purchasing the devices. In addition, the cost of periodic equipment maintenance is reduced. Among the proposed solutions to reduce chattering and improve SMC performance, we find terminal SMC (TSMC) technique [8], synergetic control [9], integral SMC (ISMC) strategy [10], fast TSMC technique [11], adaptive global SMC control [12], total SMC [13], nonsingular TSMC [14], fast TSMC technique [15], and fast integral TSMC [16].

Traditionally, the terminal SMC (TSMC) command was proposed in 1996 by Yu et al. [17]. Compared to that of the classical SMC technique, TSMC offers some superior characteristics such as high steady-state tracking precision and fast and finite-time convergence, such as motor control, robot command, multiagent systems, stochastic nonlinear systems, second-order SMC command, TSMC observer, and distributed command. Nevertheless, the TSMC command technique has a singularity problem. The latter is among the biggest obstacles that limit the use of the TSMC method. In [18], a nonsingular fast TSMC technique was proposed for position tracking of the electric cylinder. ASG control through rotor current controllers proposed by the TSMC technique is designed in [19], and in this work, the current and torque undulations are reduced compared to the classical method. A super twisting fractional-order terminal SMC technique was designed to command the rotor converter of ASG [20]. In [21], the rotor side converter of ASG is controlled by using the second-order integral TSMC method. The TSMC approach improves the performance of the ASG-based wind turbine compared to a standard SMC method [22].

In recent decades, several new methods were published with the goal of overcoming the chattering phenomenon of classical SMC techniques. In [23], an approach of the high-order SMC technique was designed. In [24], another approach was designed to overcome the problem of the high-order SMC technique. These two techniques adopted indirect methods to overcome the problem of the chattering phenomenon. In [25], the author uses the super twisting algorithm (STA) to control the induction generator. The neural algorithm and the STA technique were combined to reduces voltage and stator current ripples of ASG-based wind power [26]. The combination of the STA algorithm and the neuro-fuzzy methods was completed to obtain a more robust method, as well as to reduce oscilations at the level of electromagnetic torque and active power [27]. STA algorithm with fuzzy logic was used to control doubly fed induction machines [28]. In [29], a direct power control (DPC) with the STA algorithm minimized the ripples of active power compared to that of DPC with a look-up table. In [30], the author uses the STA algorithm to command the power of the synchronous generator (SG). In [31], the fractional order-based super twisting algorithm (FOSTA) improves the performances of the BLDC compared to that of proportional-integral (PI) controllers. The STA technique minimizes the chattering effect, which is inherent in the traditional SMC method [32,33]. In [34], the adaptive intelligent global SMC method was proposed to minimize the current ripple of a DC-DC buck inverter. In [35], the DPC strategy was designed based on the variable gain STA technique to command ASG-based wind turbines. In [36], the STA improves the performance of the DFIG and the quality of output power compared to classical SMC control.

There is another method that was suggested in several scientific works to ameliorate the characteristics of the SMC method under the name of second-order continuous SMC method. This method is characterized by simplicity and durability, and it can be accom-

plished easily. This method is used to ameliorate the effectiveness and efficiency of the DPC and DTC of the asynchronous generator [37,38]. Synergetic control and the SMC method are combined to minimize the chattering phenomenon and ameliorate the characteristics of the quality current of the ASG [39]. This designed strategy is a simple nonlinear technique that can reduce the total harmonic distortion (THD) of current compared to that of the traditional strategy. To obtain lower current ripples and high-quality energy efficiency, a new nonlinear strategy is designed in [40]. This designed new strategy is simple and gives very excellent results compared with that of the PI controller. This method was called terminal synergetic control.

There are many nonlinear methods proposed to ameliorate the purity of current produced from renewable sources. All these methods have one goal: to obtain good results in terms of ripples of effective power, electric current, and THD value.

In this work, we attempt to deliver a new method for SMC to reduce the chattering phenomenon as well as improve the performance and efficiency of the asynchronous generator-based contra-rotating wind turbine power (CRWP). This method will be called below as the third-order sliding mode (TOSM) command. This new method is the main contribution made in this paper.

In this work, the TOSM command was designed to control and minimize the ripples of current, reactive power, torque, and active power of ASG-based variable- speed CRWP systems. A TOSM technique to overcome the undulations power problem is designed for the direct field-oriented control (DFOC) technique of variable-speed CRWP systems. A DFOC control strategy with TOSM controllers is employed to enable avoidance of the power undulations and improve the response time. The system states can be ensured to improve in variation parameters. The principle of the proposed TOSM controllers is detailed in the work. Validation of the designed technology is carried out by digital simulations using Matlab software.

In summary, the novelties and main findings of this paper are as follows:

- A new TOSM controller based on the DFOC control scheme is proposed to reduce ripples of both reactive and active powers.
- TOSM controllers minimize the tracking error for reactive and active powers towards the references of ASG-based variable speed CRWP systems.
- The DFOC-TOSM control scheme with the PWM technique minimizes the THD value of torque, voltage, and active power of ASG-based variable speed CRWP.

Thus, the combination of the work is as follows. In Section 2, contra-rotating wind turbine system models are presented. In Section 3, the proposed nonlinear controller is presented using the STA controller. Section 4 includes the DFOC control scheme with designed controllers. Section 5 presents and discusses the numerical results of the research carried out.

2. CRWP Model

Wind energy is inexhaustible, clean, does not require much maintenance, and is inexpensive. The use of wind energy is now common in the world in the field of electric energy generation. The most widely used generation system for wind power conversion is the single-turbine, which is capable of converting 59% of the total wind power into useful electrical power [41]. This is still a very small percentage and needs to be increased. In order to ameliorate the characteristics and development of a single-rotor system, there are several scientific types of research in this regard to increase the efficiency of power recovery. Among these most effective solutions, we find the two-rotor system or contra-rotating wind power. The latter can increase the power conversion efficiency by 40% compared to that of a single turbine system (STS) [42]. This new method is explained in [43–47]. In this new technology, two turbines were used to raise and increase the ability to collect energy from the wind. Experiments proved the effectiveness of this new technology. However, the first is a small turbine and the second is a large turbine. The difference between new and old technology lies in the number of mechanical components and the amount of energy gained

from the wind. As is known through the scientific experiments conducted on this new technology, all the results are in favor of the new technology. Besides, this new turbine has excellent characteristics in regions with high and low wind speeds. Among its advantages is that it operates at lower tip speed ratios compared to that of the traditional STS [47]. However, this method has several disadvantages, such as high costs, control difficulties, and risk of subsynchronous resonance. On the other hand, the new technology has more mechanical components than the classic wind turbine. The mechanical energy obtained from this new technology is shown in Equation (1). Through this equation, the total energy of this technology is the sum of the two energies of the small and large turbines:

$$P_{CRWP} = P_T = P_{ST} + P_{LT} \tag{1}$$

where P_{ST} and P_{LT} are the mechanical power of the small and large turbines.

In the CRWP system, the resulting aerodynamic torque is the sum of the torques of the small and large turbines and is represented by the Equation (2).

$$T_{CRWP} = T_T = T_{ST} + T_{LT} \tag{2}$$

where T_{ST} and T_{LT} are the aerodynamic torque of the small and large turbines.

Equations (3) and (4) represent the aerodynamic torque for of the large and small turbines [45].

$$T_{LT} = \frac{C_p}{2 \cdot \lambda_{LT}^3} \cdot \rho \cdot \pi \cdot R_{LT}^5 \cdot w_{LT}^2 \tag{3}$$

$$T_{ST} = \frac{C_p}{2 \cdot \lambda_{ST}^3} \cdot \rho \cdot \pi \cdot R_{ST}^5 \cdot w_{ST}^2 \tag{4}$$

where: R_{ST} and R_{LT} are the blade radius of the small and large turbines; ρ: the air density; λ_{ST}, λ_{LT}: the tip speed ration of the small and large turbines; w_{ST}, w_{LT} the mechanical speed of the small and large turbines.

Equations (5) and (6) represents the tip speed ratios of the small and large turbines, respectively.

$$\lambda_{ST} = \frac{w_{ST} \cdot R_{ST}}{V_{ST}} \tag{5}$$

$$\lambda_{LT} = \frac{w_{LT} \cdot R_{LT}}{V_{LT}} \tag{6}$$

where V_{ST} and V_{LT} are the speed of the unified wind on small and large turbines.

To calculate the wind speed at a point between a large and a small turbine, we use Equation (7). Fifteen m is the distance (x) between the center of the large turbine and the center of the small turbine [48].

$$V_x = V_{LT} \cdot \left(1 - \frac{1 - \sqrt{1 - C_T}}{2} \cdot (1 + \frac{2 \cdot x}{\sqrt{1 + 4 \cdot x^2}})\right) \tag{7}$$

where C_T is the trust coefficient (C_T = 0.9) and Vx is the wind speed at a point between a large and small turbine.

Cp in terms of the pitch angle (β) is given by Equation (8) [49].

$$C_p(\beta, \lambda) = 0.517 \cdot \left(\frac{116}{\lambda_i} - 0.4 \cdot \beta - 5\right) \cdot e^{\frac{-21}{\lambda_i}} + 0.0068 \cdot \lambda \tag{8}$$

3. Third-Order Sliding Mode Control

There are many types of SMC techniques in the literature. All these proposed methods aim to reduce chattering phenomena. The one with the simplest algorithm and the easiest experimentally is the STA method [50,51]. This method was applied in several fields, for example, electronic and electrical control. In [52], there are two types of STA which are

as follows: super twisting extended state observer and super twisting SMC. These two methods were applied to wind turbines to compare them. In [53], the characteristic of DFOC was improved by the STA method. Experimental results showed the characteristics of the STA technique in improving the response time of a six-phase motor. STA technique was proposed to control the DC-link of the NPC inverter [54]. Internal permanent-magnet synchronous motors (IPMSMs) were controlled by an adaptive STA observer [55]. In [56], the author proposes to use the STA technique to command the output current of the multilevel converter. Permanent-magnet synchronous motors (PMSMs) were controlled by two different types of nonlinear controllers (STA and SMC) [57]. Experimental results showed that the STA improved the motor properties compared to that of SMC. In [58], the author proposes to use the STA technique to control the photovoltaic system. The STA technique has a very high efficacy compared to that of the classical method, as seen in the results of [58]. Synchronous motors (SMs) were controlled by the STA method [59]. STA observer with adaptive parameters estimation was proposed to command the IPMSMs [60]. In [61], the author proposes to use the STA technique to control the DC motor. The numerical simulation results showed that the characteristics of the STAR technique improve the performance and efficiency of the DC motor.

In this section, a new technique to reduce the chattering phenomena and minimizes the ripples of active power and current for ASG-CRWP was designed. The designed technique, named third-order sliding mode (TOSM), is an effective method for uncertain systems to overcome the main drawbacks of the classical SMC technique and STA described in the literature. The proposed strategy is a nonlinear method based on the STA method. The command input of the designed TOSM controller comprises three inputs given by Equation (9):

$$u(t) = u_1(t) + u_2(t) + u_3(t) \tag{9}$$

$$u_1(t) = \lambda_1 \cdot \sqrt{|S|} \cdot Sign(S) \tag{10}$$

$$u_2(t) = \lambda_2 \cdot \int Sign(S)dt \tag{11}$$

$$u_3(t) = \lambda_3 \cdot Sign(S) \tag{12}$$

Equation (13) shows the output of the proposed TOSM method:

$$u(t) = \lambda_1 \cdot \sqrt{|S|} \cdot Sign(S) + \lambda_2 \cdot \int Sign(S)dt + \lambda_3 \cdot Sign(S) \tag{13}$$

The tuning constants λ_1, λ_2, and λ_3 are used to refine the TOSM strategy for controller smoothing.

This suggested method was used to improve the performance of the DFOC method. Figure 1 shows the structure of the proposed TOSM controller.

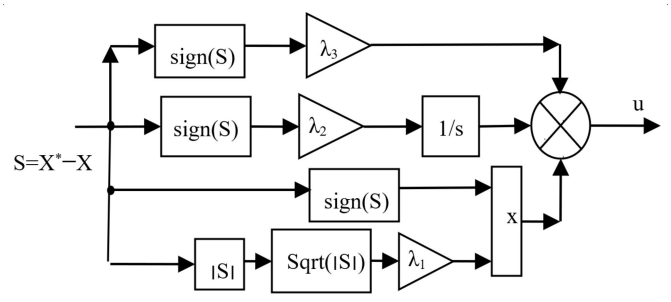

Figure 1. Structure of proposed TOSM controller.

The stability condition is given by:

$$S \cdot \dot{S} < 0 \tag{14}$$

This TOSM technique is designed in this work to minimize the ripple of stator current, active power, electromagnetic torque, and reactive power in an ASG-based CRWP system using the DFOC strategy and an inverter controlled by the classical PWM technique.

4. DFOC-TOSM Control

In the literature, the FOC technique was widely used for AC machines. The principle of this control is to orient the stator flux along the axis of the rotating frame. Two types of FOC strategies were studied in literature: direct and indirect FOC control. Traditional FOC control was proposed to control the induction generator [62]. In [63], the indirect FOC (IFOC) technique improved the performance of the induction generator compared with that of the DFOC technique. In [64], the FOC strategy was designed based on the neuro-fuzzy (NF) controllers to minimize the current and flux of the ASG. The experimental result shows the superiority of the designed FOC-NF technique. In [65], the FOC strategy was designed based on SVM technique and hysteresis current to minimize the reactive power ripples of ASG-based traditional wind power.

In this section, we propose to ameliorate the performances of the DFOC strategy of the asynchronous generator integrated into the CRWP system. This method is based on the following principle [64]:

$$\psi_{ds} = 0 \text{ and } \psi_{qs} = \psi_s \tag{15}$$

Hence, direct stator voltage and quadrature stator voltage can be written as:

$$\begin{cases} V_{qs} = V_s = w_s \cdot \psi_s \\ V_{ds} = 0 \end{cases} \tag{16}$$

Equation (17) expresses each of direct stator current and quadrature stator current of the induction generator.

$$\begin{cases} I_{qs} = -\frac{M}{L_s} \cdot I_{qr} \\ I_{ds} = -\frac{M}{L_s} \cdot I_{dr} + \frac{\psi_s}{L_s} \end{cases} \tag{17}$$

The active and reactive power are obtained from Equation (18).

$$\begin{cases} Q_s = -1.5\left(\frac{\omega_s \cdot \psi_s \cdot M}{L_s} \cdot I_{dr} - \frac{\omega_s \cdot {\psi_s}^2}{L_s}\right) \\ P_s = -1.5\frac{\omega_s \cdot \psi_s \cdot M}{L_s} \cdot I_{qr} \end{cases} \tag{18}$$

Equation (19) represents the torque.

$$T_{em} = -1.5\ I_{qr} \cdot\ \psi_{ds} \cdot\ p \cdot \frac{M}{L_s} \tag{19}$$

Equation (20) expresses each of direct rotor voltage and quadrature rotor voltage of the induction generator.

$$\begin{cases} V_{qr} = R_{dr} \cdot I_{qr} + \left(L_r - \frac{M^2}{L_s}\right) p \cdot I_{qr} - g \cdot w_s \left(L_r - \frac{M^2}{L_s}\right) I_{dr} + g \cdot \frac{M \cdot V_s}{L_s} \\ V_{dr} = R_{dr} \cdot I_{dr} + \left(L_r - \frac{M^2}{L_s}\right) \cdot p \cdot I_{dr} - g \cdot w_s \cdot \left(L_r - \frac{M^2}{L_s}\right) \cdot I_{qr} \end{cases} \tag{20}$$

Equation (21) represents direct and quadrature rotor current of the ASG.

$$\begin{cases} I_{qr} = \left(V_{qr} - g \cdot w_s \cdot \left(L_r - \frac{M^2}{L_s}\right) \cdot I_{qr} - g \cdot \frac{M \cdot V_s}{L_s}\right) \cdot \frac{1}{R_r + \left(L_r - \frac{M^2}{L_s}\right) \cdot p} \\ I_{dr} = \left(V_{dr} - g \cdot w_s \left(L_r - \frac{M^2}{L_s}\right) \cdot I_{qr}\right) \cdot \frac{1}{R_r + \left(L_r - \frac{M^2}{L_s}\right) \cdot p} \end{cases} \tag{21}$$

The DFOC method is a very simple and easy to implement method, and it can be applied to any electric machine. In addition, it is inexpensive compared to that of other methods. The principle of this method can be expressed as in Figure 2. From this figure, it

is observed that two independent PI controllers to control the direct and quadrature rotor voltages are used.

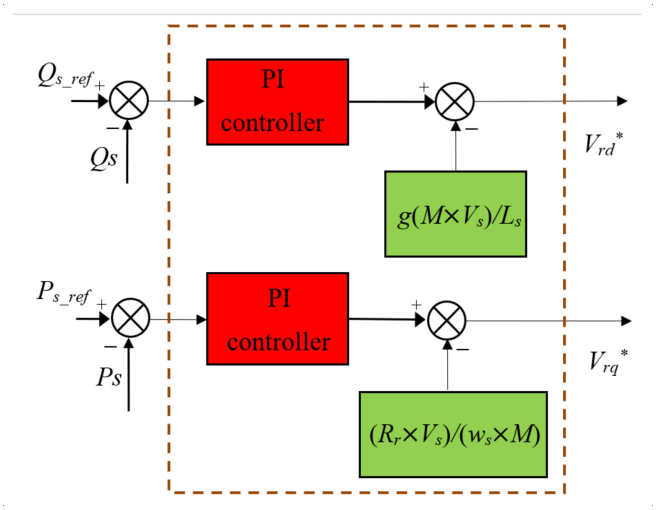

Figure 2. Classical DFOC strategy.

This method is simple but provides greater ripples for both current and active power. Also, the response time is rather large compared, for example, with direct power command (DPC) and direct torque command (DTC), and this is due to the use of PI controllers.

In this paper, we propose to ameliorate the characteristics and effectiveness of this method by the proposed nonlinear TOSM method. Thus, by improving the quality of the current produced, the life of the generator and the system as a whole is extended as well.

The principle of the TOSM-DFOC strategy is the direct regulation of the current, active power, voltage, torque, and reactive power of the ASG-based CRWP system by using two TOSM techniques. The two regulated variables are reactive and active powers, which are usually controlled by TOSM controllers. The idea is to keep the active and reactive power quantities within the designed sliding surfaces.

The DFOC with TOSM controllers (TOSM-DFOC) is a modification of the traditional DFOC strategy, where the PI regulators were replaced by TOSM controllers, as shown in Figure 3.

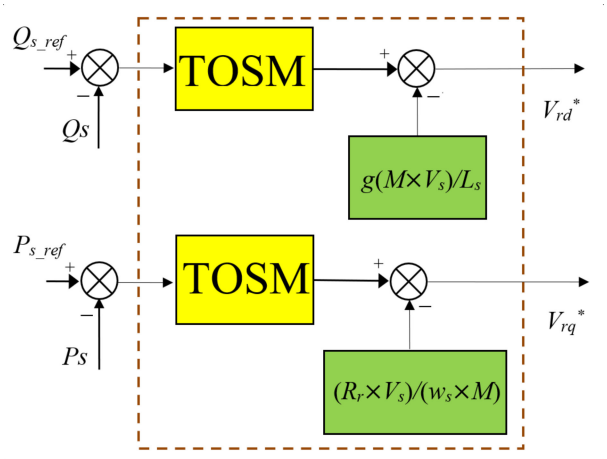

Figure 3. Structure of DFOC-TOSM strategy.

The TOSM technique was designed to force the regulated dynamics towards manifolds and keeps them there. To force the ASG active and reactive powers to track their corresponding references, the sliding surfaces S_{Qs} and S_{Ps} of the reactive and active powers

are selected as the error between the desired and real dynamics, being given by Equations (22) and (23), respectively:

$$S_{Ps} = P_s^* - P_s \tag{22}$$

$$S_{Qs} = Q_s^* - Q_s \tag{23}$$

The sliding surfaces shown in Equations (22) and (23) are used as inputs for the TOSM command law. Thus, TOSM regulators for the active and reactive power are used to influence the two rotor voltage components, as in Equations (24) and (25), respectively:

$$V_{dr}^* = \lambda_1 \cdot \sqrt{|S_{Qs}|} \cdot Sign(S_{Qs}) + \lambda_2 \cdot \int Sign(S_{Qs})dt + \lambda_3 \cdot Sign\ (S_{Qs}) \tag{24}$$

$$V_{qr}^* = \lambda_1 \cdot \sqrt{|S_{Ps}|} \cdot Sign(S_{Ps}) + \lambda_2 \cdot \int Sign(S_{Ps})dt + \lambda_3 \cdot Sign(S_{Ps}) \tag{25}$$

This proposed technique is implemented for a DFOC strategy based on the TOSM controllers to obtain minimum active power undulations and to minimize the chattering phenomenon. The controller structure of the TOSM technique for the reactive and active powers of the DFOC strategy is presented in Figures 4 and 5, respectively.

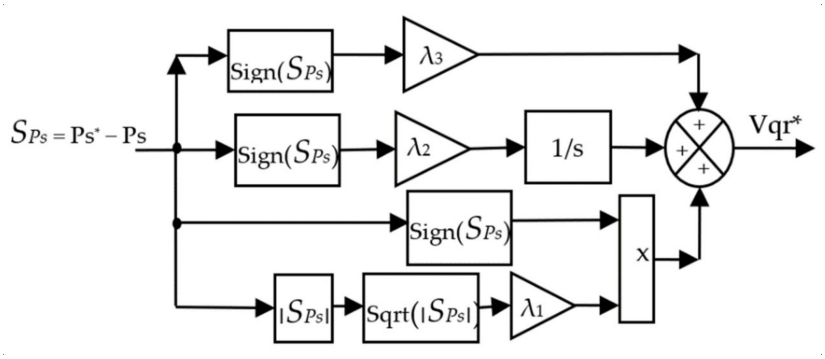

Figure 4. Proposed TOSM active power controller.

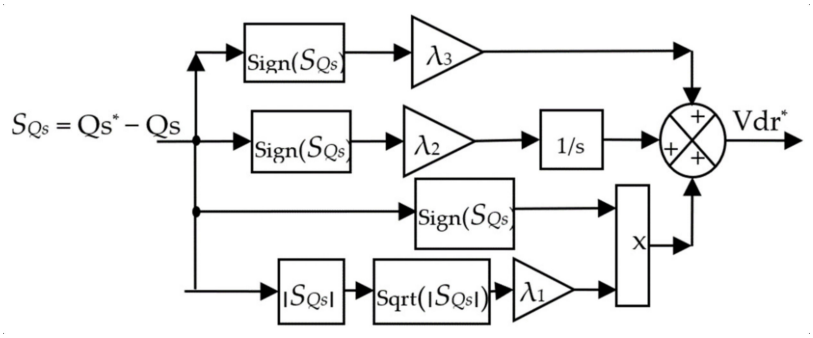

Figure 5. Proposed TOSM reactive power controller.

The basic block diagram of the DFOC-TOSM strategy is shown in Figure 6. This strategy is designed as a simple algorithm that provides a robust command. However, this proposed strategy gives a fast response dynamic compared to DFOC, DPC, and DTC. This designed technique can better minimize the active and reactive power undulations compared to that of classic DPC, DFOC, and DTC strategies.

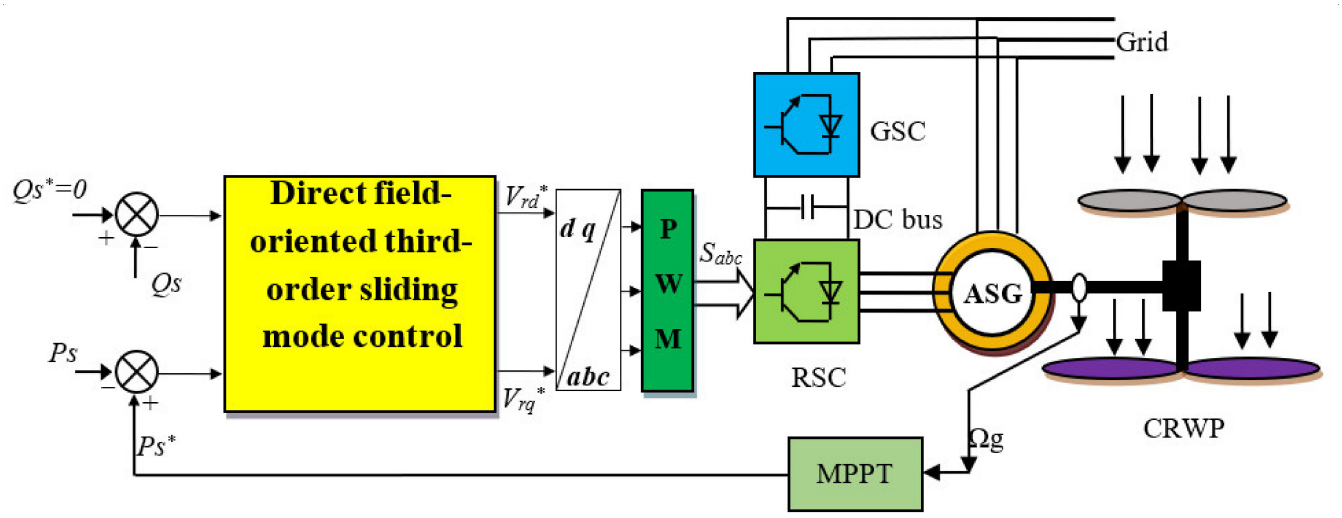

Figure 6. DFOC-TOSM control of ASG-CRWP.

The proposed method is one of the best methods available today, and this is due to the use of TOSM. The following table (Table 1) shows a comparative study between the proposed method and some of most famous and widely used methods, such as DTC, DPC, and FOC control scheme. From Table 1, we note that the proposed method is more robust than the rest of the methods in terms of improving the dynamic response and THD value. But this method is rather complicated compared to that of the classic DTC and DPC.

Table 1. A comparative study between DFOC-TOSM with some techniques.

Control Techniques	Controller	Complexity	Current Oscillations	Reference Tracking	Dynamic Responses	Sensitivity to Parameter Change	THD (%) of Current
DTC control	Hysteresis controller	Low	High	Good	Good	High	High
DPC control	Hysteresis controller	Low	High	Good	Good	High	High
FOC control	PI	High	High	Acceptable	Acceptable	High	High
Proposed technique (DFOC-TOSMC)	TOSM controller	High	Low	Excellent	Excellent	Medium	Low

5. Numerical Simulation

The proposed TOSM controller as applied for the ASG reactive and active powers was implemented using MATLAB® software. Comparison between the proposed method and the classical PI controller in terms of current, active power, torque and reactive powers undulations reduction, wind speed changing, trajectory tracking, and robustness to ASG parameter variations.

The generator used in the digital simulation has the following characteristics: f = 50 Hz, p = 2, Rs = 0.012 Ω, Lr = 0.0136 H, Pn = 1.5 MW, Rr = 0.021 Ω, Ls = 0.0137 H, Vn = 380 V, J = 1000 K×gm^2, M = 0.0135 H, F = 0.0024 N×m.

The grid used in the simulation has the following parameters: nominal grid voltage (Vg = 389 V), nominal grid frequency (fs = 50 Hz), DC-link voltage (E = 1200 V), filter inductance (Lg = 6 mH), and filter resistance (Rg = 0.15 Ω).

DFOC with PI controllers (DFOC-PI) and DFOC-TOSM are simulated and compared in terms of current, reactive power, torque and active power undulations, reference tracking, and THD value of current.

To test the effectiveness and robustness of the proposed method, we proposed two different tests: the first is related to tracking the trajectory and the second to assess the robustness to changes in some parameters of the machine.

5.1. First Test

The results obtained from the simulation for the two methods are shown in Figures 7–12. In the case of each of the two proposed methods, the measured values of reactive and active power follow the reference values very well (see Figures 9 and 10). On the other hand, for the two techniques, the active and reactive powers perfectly track their references values, for which the TOSM controller introduces better performances in terms of settling time, overshoot damping, and steady-state error decreasing. In Figures 9 and 10, both controllers introduce a good tracking performance with a remarkable superiority of the proposed TOSM controller in terms of rise time, settling time, and steady-state error, which all decrease. The electric current has the form of active power and is related to the wind speed, as seen in Figure 12.

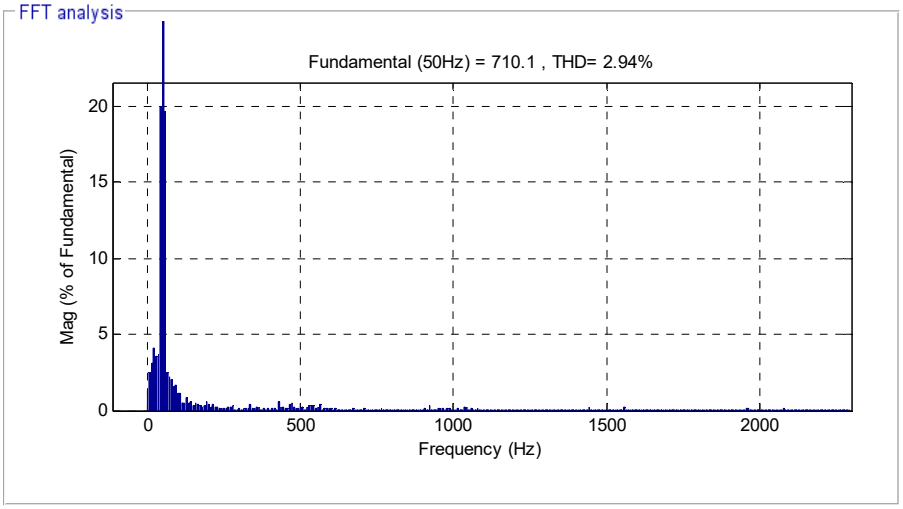

Figure 7. THD (DFOC-PI).

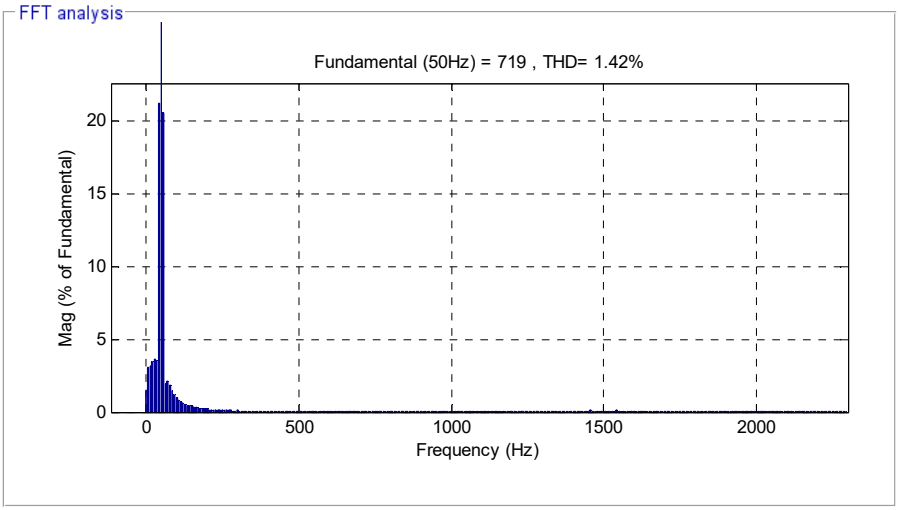

Figure 8. THD (DFOC-TOSM).

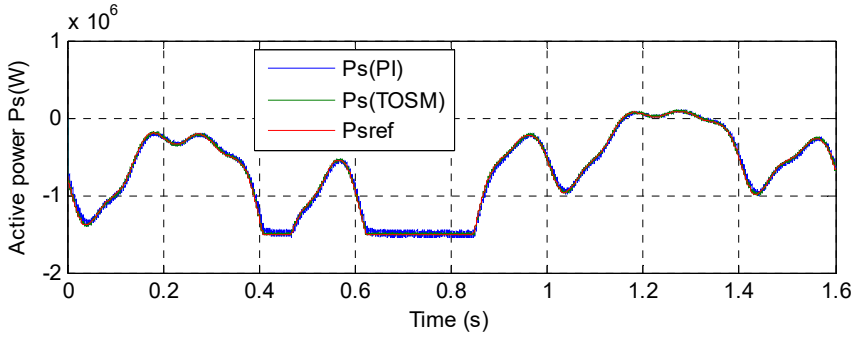

Figure 9. Active power.

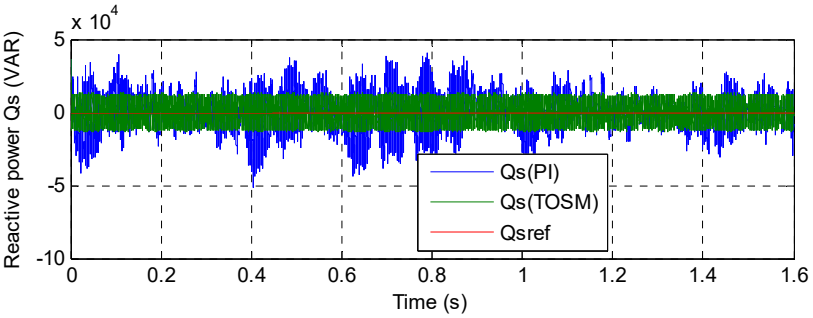

Figure 10. Reactive power.

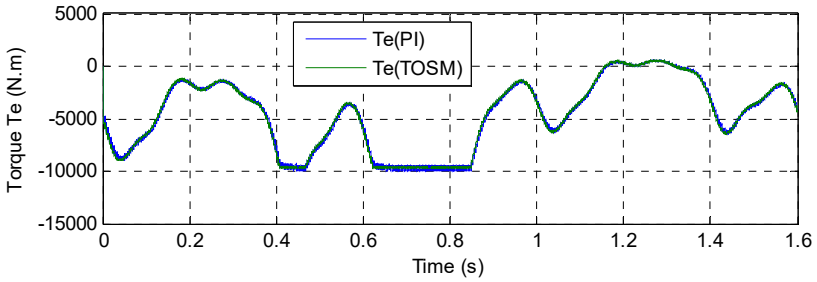

Figure 11. Torque.

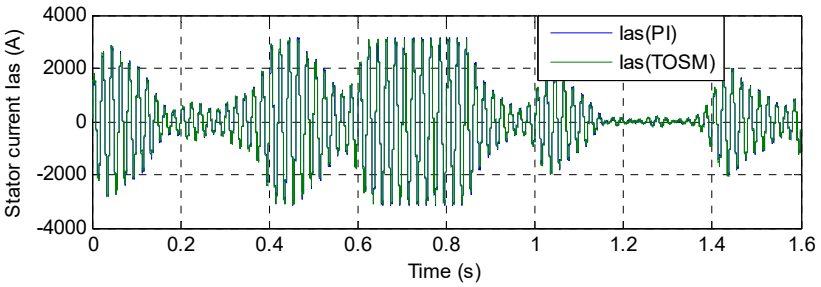

Figure 12. Current.

The torque resulting from the two proposed methods is shown in Figure 11. From this figure, we find that the value of the torque is related to the values of active power and wind speed. To further compare the characteristics of these two techniques, the stator currents harmonic spectra are compared.

Figures 7 and 8 show the THD of stator current of the AG-CRWP system for both DFOC strategies. Here, the THD value is reduced for the DFOC-TOSM (1.42%) when compared to that of the DFOC-PI (2.94%). The THD reduction can be estimated at 51.71%.

The zoom in the current, active power, and torque is shown in Figures 13–15, respectively. The DFOC-TOSM strategy reduces the undulations in torque, reactive power,

current, and active power compared to that of the DFOC-PI strategy, and the reduction rate is estimated at 84%, 94.5%, 78%, and 90%, respectively, compared to that of the classical method (DARPC). Based on the results above, the DFOC-TOSM strategy proved its efficiency in minimizing undulations and chattering phenomena.

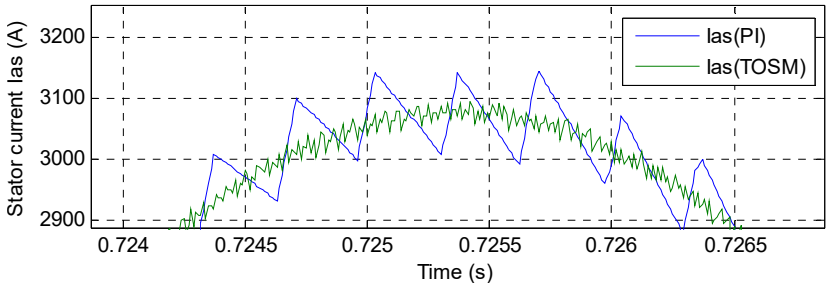

Figure 13. Zoom (Current).

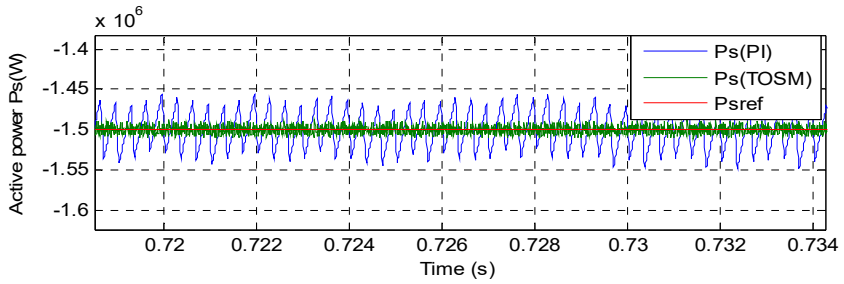

Figure 14. Zoom (Active power).

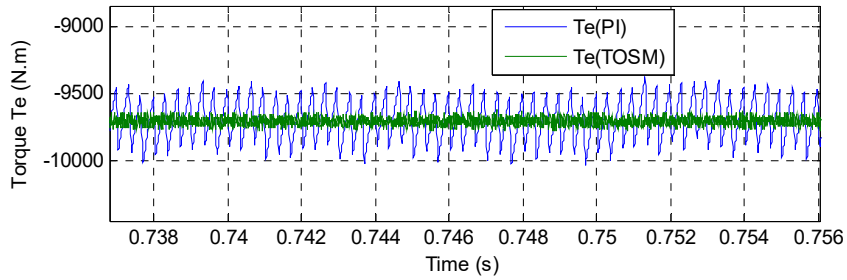

Figure 15. Zoom (Torque).

5.2. Second Test

The aim of this test is to find out which method is not affected by changing the following parameters: *Rs*, *Rr*, *Ls*, *M*, and *Lr*. Figures 16–21 show the simulation results for variations in inductance and resistance values. Note that there is a change in reactive power, torque, active power, and current because both active power and torque are related to changing values of parameters. The classical technique was heavily affected by the change of parameter values compared to that of the designed technique (Figures 22–24), and this is evident in the value of THD (Figures 16 and 17). The ripple reduction can be estimated at 73.94%. Parameter changes have a clear effect on the dynamic performances of active power, current, torque, and stator reactive power when using the PI controller. In addition, the decoupling between the reactive and active powers is not ensured in this case. Instead, the designed DFOC based TOSM controller is robust against parameter variations, and decoupling is perfectly ensured.

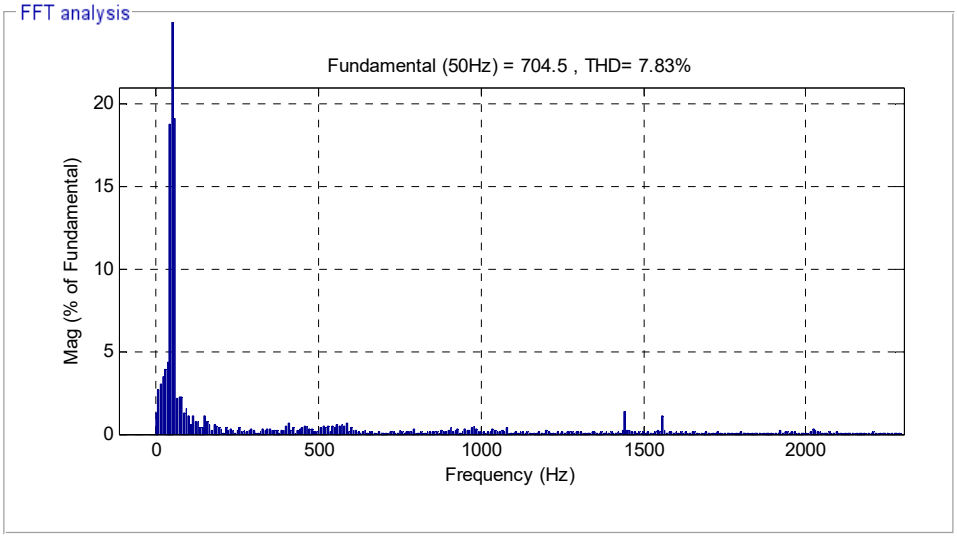

Figure 16. THD (PI-DFOC).

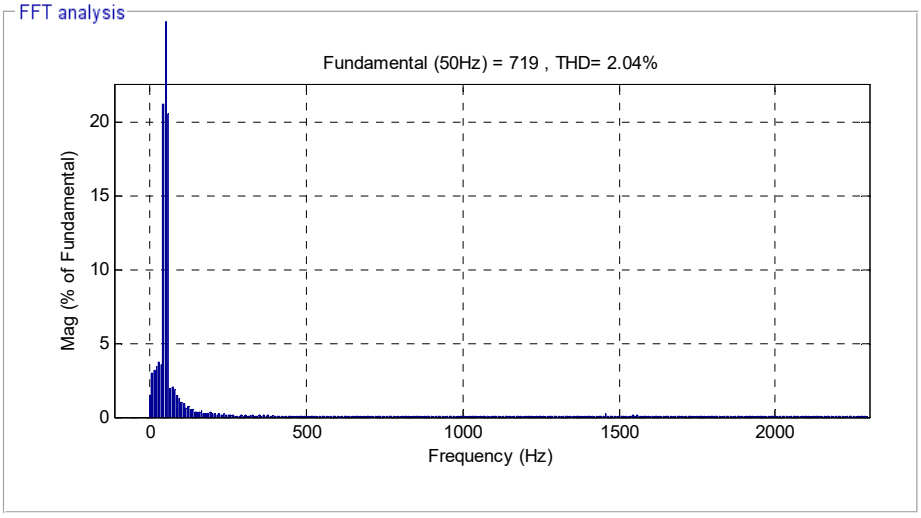

Figure 17. THD (TOSM-DFOC).

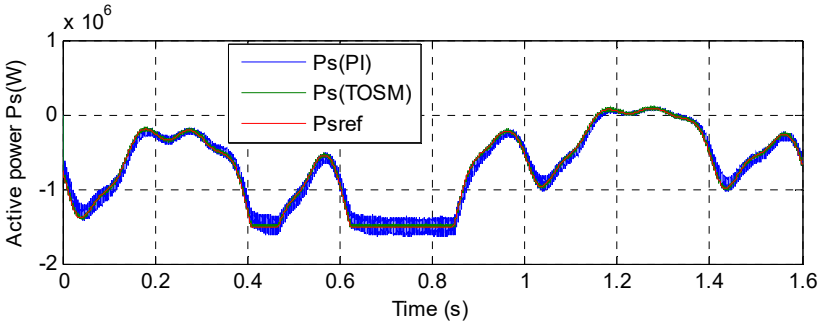

Figure 18. Active power.

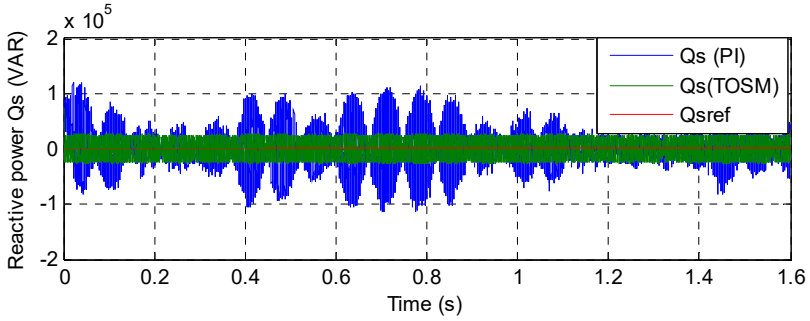

Figure 19. Reactive power.

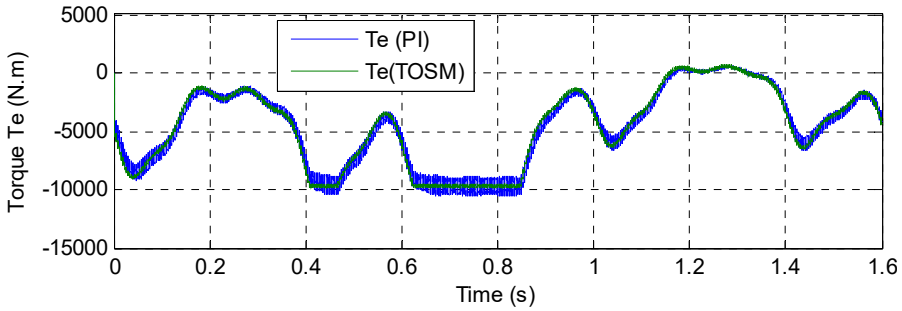

Figure 20. Torque.

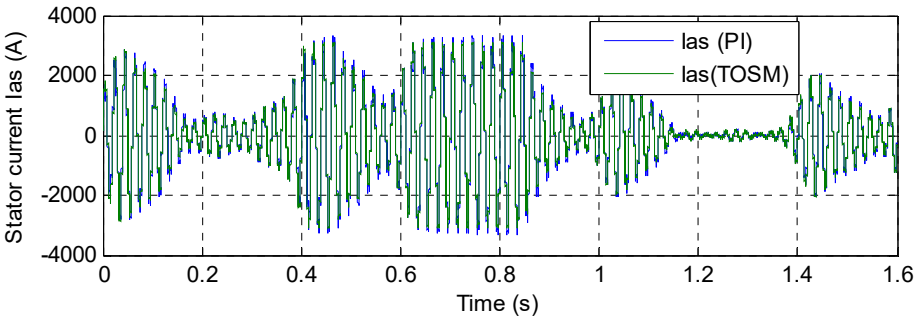

Figure 21. Current.

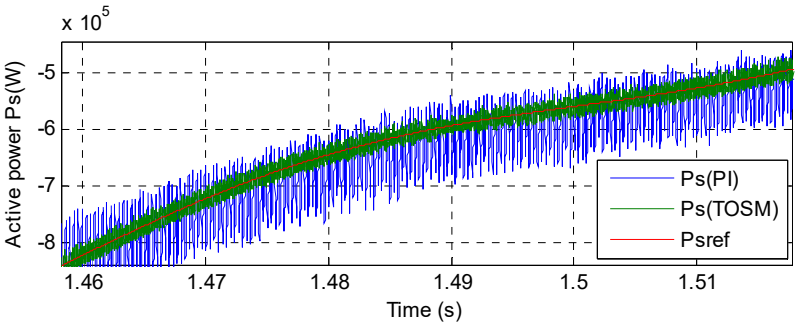

Figure 22. Zoom (Active power).

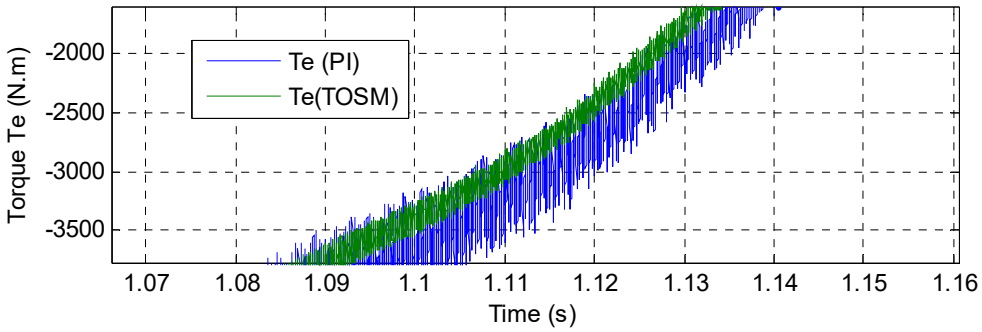

Figure 23. Zoom (Torque).

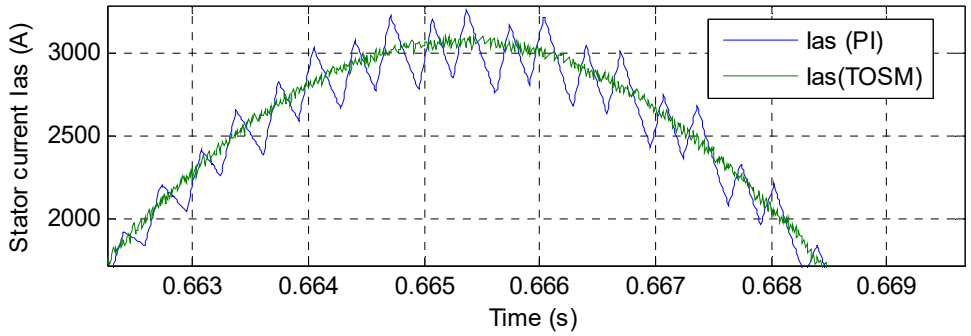

Figure 24. Zoom (Current).

Thus, the DFOC with designed TOSM algorithms is more robust than the classical DFOC technique.

The obtained results can be summarized in Table 2. Table 2 presents a comparative study between the proposed method and the classical method in all respects. Through this table, we note that the proposed method gave very satisfactory results in terms of reducing the torque and flux fluctuations. Also, the proposed method improved the dynamic response compared to that of the classical method. On the other hand, the proposed method provided better results in terms of current, reactive power, torque and active power fluctuations, reactive and active power tracking, and the quality of the produced current. The proposed DFOC-TOSM technique is more robust than that of the traditional DFOC using PI controllers except for the dynamic response, rise time, overshoot, and settling time, which is faster in the proposed technique than that of the DFOC technique. However, the proposed technique is complicated relative to the calculations to be performed compared to that of the DFOC control technique.

A comparative study between the proposed method in this paper with some published works in terms of the value of THD is presented in Table 3. Through this table, the proposed method provided a very good THD value of the current compared to that of the rest of the other controls. Tables 2 and 3 show that the proposed method is more robust and can be used to improve the quality of current and energy produced from the wind power generation system.

Table 2. Comparative results obtained from DFOC-TOSM with DFOC control.

Criteria	Control Techniques	
	DFOC	**DFOC-TOSM**
Reactive and active power tracking	Well	Excellent
THD (%)	2.94	1.42
Reactive and active power ripples	Acceptable	Excellent
Dynamic response (s)	Medium	Fast
Reactive power: ripples (VAR)	Around 20,000	Around 1100
Torque: ripple (N.m)	Around 500	Around 80
Settling time (ms)	High	Medium
Overshoot (%)	Remarkable ≈ 19%	Neglected ≈ 1.5%
Sensitivity to parameter change	High	Medium
Active power: ripples (W)	Around 10,000	Around 1000
Simplicity of converter and filter design	Simple	Simple
Rise Time (s)	High	Medium
Stator current ripple (VAR)	Around 100	Around 22
Simplicity of calculations	Simple	Rather complicated
Improvement of transient performance	Good	Excellent
Quality of stator current	Acceptable	Excellent

Table 3. Comparative results with other methods.

References	Techniques	THD (%)
Ref. [6]	Fuzzy SMC technique	3.05
Ref. [38]	Direct torque command	2.95
Ref. [64]	FOC with hysteresis current controller	3.70
Ref. [66]	Virtual flux DPC method	4.19
	DPC	4.88
Ref. [67]	Integral SMC technique	9.71
	Multi-resonant-based sliding mode controller (MRSMC)	3.14
Ref. [68]	SOSMC method	3.13
Ref. [69]	DPC control with STA controller	1.66
Designed strategies	DFOC-PI	2.94
	DFOC-TOSM	1.42

6. Conclusions

In this study, a new TOSM strategy was designed to command the generated reactive and active power from the ASG based on the variable speed CRWP. The designed strategy aims to ameliorate the command characteristics of the algorithm that are based on the proposed TOSM methods by minimizing active power, torque, current, and reactive power undulations under variable speed CRWP system.

The proposed TOSM command was used to define the attractive command section of the classic SMC strategy.

The designed strategy was compared with that of the classical PI controller. The obtained results illustrated the effectiveness of the designed TOSM strategy, even in the presence of time-varying reference trajectory, ASG parameter variations, and changes in speed wind. Current, active power, torque, and reactive power undulations were largely

minimized, and response time was improved using the designed TOSM strategy. Moreover, robustness, stability, and high-decoupling between the command axes were ensured.

The simulation results showed that the introduced TOSM-based DFOC control scheme is high performance and has a robustness to uncertainties and parameter mismatches as well as the attenuation of chattering phenomena in comparison with that of the DFOC control scheme-based conventional PI controllers. The designed control technique improved the active power ripple, current ripple, torque ripple, reactive power ripple, and THD value of stator current by about 90%, 78%, 84%, 94%, and 51.71%, respectively, compared to that of the classic DFOC strategy. Finally, the designed TOSM strategy may be a good solution to improve the DFOC strategy effectiveness applied for power systems, ensuring high quality of active power and stator current.

To summarize, the main findings of this research are as follows:

- A novel nonlinear controller was presented and confirmed with numerical simulation.
- A new DFOC strategy based on the proposed TOSM algorithm was presented and confirmed with numerical simulation.
- A robust command technique was designed to minimize the ripples of current, active power, electromagnetic torque, and reactive power.
- The THD value of stator current was reduced by the proposed strategy.

In future work, to improve the quality of the voltage, torque, current, and active power, the asynchronous generator will be controlled using another combination of intelligent algorithms, such as type-two fuzzy logic and neural algorithm used for DFIG in [34]. The ratio between the obtained performance and the complexity of the control will be evaluated.

Author Contributions: Validation, N.B.; conceptualization, H.B.; software, H.B.; methodology, H.B.; investigation, H.B.; resources, H.B. and N.B.; project administration, N.B.; data curation, N.B.; writing—original draft preparation, H.B.; supervision, N.B.; visualization, N.B.; formal analysis, N.B.; funding acquisition, N.B.; writing—review and editing, N.B. and H.B. All authors have read and agreed to the published version of the manuscript.

Funding: This research received no external funding.

Institutional Review Board Statement: Not applicable.

Informed Consent Statement: Not applicable.

Data Availability Statement: Not applicable.

Conflicts of Interest: The authors declare no conflict of interest.

References

1. Xiong, L.; Li, P.; Li, H.; Wang, J. Sliding Mode Control of DFIG Wind Turbines with a Fast Exponential Reaching Law. *Energies* **2017**, *10*, 1788. [CrossRef]
2. Levant, A. Robust exact differentiation via sliding mode technique. *Automatica* **1998**, *34*, 379–384. [CrossRef]
3. Rezaei, M.M. A nonlinear maximum power point tracking technique for DFIG-based wind energy conversion systems. *Eng. Sci. Technol. Int. J.* **2018**, *21*, 901–908. [CrossRef]
4. Hu, J.; Nian, H.; Hu, B.; He, Y.; Zhu, Z.Q. Direct active and reactive power regulation of DFIG using sliding-mode control approach. *IEEE Trans. Energy Convers.* **2010**, *25*, 1028–1039. [CrossRef]
5. Benbouhenni, H. Sliding mode with neural network regulateur for DFIG using two-level NPWM strategy. *Iran. J. Electr. Electron. Eng.* **2019**, *15*, 411–419.
6. Boudjema, Z.; Meroufel, A.; Djerriri, Y.; Bounadja, E. Fuzzy sliding mode control of a doubly fed induction generator for energy conversion. *Carpathian J. Electron. Comput. Eng.* **2013**, *6*, 7–14.
7. Habib, B. ANFIS-sliding mode control of a DFIG supplied by a two-level SVPWM technique for wind energy conversion system. *Int. J. Appl. Power Eng.* **2020**, *9*, 36–47. [CrossRef]
8. Abdolhadi, H.Z.; Markadeh, G.A.; Boroujeni, S.T. Sliding mode and terminal sliding mode control of cascaded doubly fed induction generator. *Iran. J. Electr. Electron. Eng.* **2021**, *17*, 1955.
9. Xiao, L.; Zhang, L.; Gao, F.; Qian, J. Robust Fault-Tolerant Synergetic Control for Dual Three-Phase PMSM Drives Considering Speed Sensor Fault. *IEEE Access* **2020**, *8*, 78912–78922. [CrossRef]
10. Hamid, C.; Aziz, D.; Seif Eddine, C.; Othmane, Z.; Mohammed, T.; Hasnae, E. Integral sliding mode control for DFIG based WECS with MPPT based on artificial neural network under a real wind profile. *Energy Rep.* **2021**, *7*, 4809–4824. [CrossRef]

11. Du, H.; Chen, X.; Wen, G.; Yu, X.; Lü, J. Discrete-Time Fast Terminal Sliding Mode Control for Permanent Magnet Linear Motor. *IEEE Trans. Ind. Electron.* **2018**, *65*, 9916–9927. [CrossRef]
12. Mobayen, S.; Bayat, F.; Lai, C.-C.; Taheri, A.; Fekih, A. Adaptive Global Sliding Mode Controller Design for Perturbed DC-DC Buck Converters. *Energies* **2021**, *14*, 1249. [CrossRef]
13. Shehata, E.G. Sliding mode direct power control of RSC for DFIGs driven by variable speed wind turbines. *Alex. Eng. J.* **2015**, *54*, 1067–1075. [CrossRef]
14. Haibo, L.; Heping, W.; Junlei, S. Attitude control for QTR using exponential nonsingular terminal sliding mode control. *J. Syst. Eng. Electron.* **2019**, *30*, 191–200. [CrossRef]
15. Wang, Z.; Li, S.; Li, Q. Discrete-Time Fast Terminal Sliding Mode Control Design for DC–DC Buck Converters with Mismatched Disturbances. *IEEE Trans. Ind. Inform.* **2020**, *16*, 1204–1213. [CrossRef]
16. Lin, X.; Shi, X.; Li, S. Adaptive Tracking Control for Spacecraft Formation Flying System via Modified Fast Integral Terminal Sliding Mode Surface. *IEEE Access* **2020**, *8*, 198357–198367. [CrossRef]
17. Yu, X.; Man, Z. Model reference adaptive control systems with terminal sliding modes. *Int. J. Control.* **1996**, *64*, 1165–1176. [CrossRef]
18. Feng, Y.; Yu, X.; Han, F. On nonsingular terminal sliding-mode control of nonlinear systems. *Automatica* **2013**, *49*, 1715–1722. [CrossRef]
19. Morshed, M.J.; Fekih, A. A terminal sliding mode approach for the rotor side converter of a DFIG-based wind energy system. In Proceedings of the 2018 IEEE Conference on Control Technology and Applications (CCTA), Copenhagen, Denmark, 21–25 April 2018; pp. 1736–1740. [CrossRef]
20. Sami, I.; Ullah, S.; Ali, Z.; Ullah, N.; Ro, J.-S. A Super Twisting Fractional Order Terminal Sliding Mode Control for DFIG-Based Wind Energy Conversion System. *Energies* **2020**, *13*, 2158. [CrossRef]
21. Morshed, M.J.; Fekih, A. Second order integral terminal sliding mode control for voltage sag mitigation in DFIG-based wind turbines. In Proceedings of the 2017 IEEE Conference on Control Technology and Applications (CCTA), Mauna Lani, HI, USA, 27–30 August 2017; pp. 614–619. [CrossRef]
22. Levant, A. Sliding order and sliding accuracy in sliding mode control. *Int. J. Control.* **1993**, *58*, 1247–1263. [CrossRef]
23. Levant, A. Higher-order sliding modes, differentiation and output-feedback control. *Int. J. Control.* **2003**, *76*, 924–941. [CrossRef]
24. Shah, A.P.; Mehta, A.J. Direct power control of DFIG using super-twisting algorithm based on second-order sliding mode control. In Proceedings of the 2016 14th International Workshop on Variable Structure Systems (VSS), Nanjing, China, 1–4 June 2016; pp. 136–141. Available online: https://ieeexplore.ieee.org/document/7506905 (accessed on 1 September 2021). [CrossRef]
25. Alhato, M.M.; Ibrahim, M.N.; Rezk, H.; Bouallègue, S. An Enhanced DC-Link Voltage Response for Wind-Driven Doubly Fed Induction Generator Using Adaptive Fuzzy Extended State Observer and Sliding Mode Control. *Mathematics* **2021**, *9*, 963. [CrossRef]
26. Habib, B.; Boudjema, Z.; Belaidi, A. Direct power control with NSTSM algorithm for DFIG using SVPWM technique. *Iran. J. Electr. Electron. Eng.* **2021**, *17*, 1–11.
27. Habib, B.; Boudjema, Z.; Belaidi, A. DPC based on ANFIS super-twisting sliding mode algorithm of a doubly-fed induction generator for wind energy system. *J. Eur. Des. Systèmes Autom.* **2020**, *53*, 69–80.
28. Farid, B.; Tarek, B.; Sebti, B. Fuzzy super twisting algorithm dual direct torque control of doubly fed induction machine. *Int. J. Electr. Comput. Eng.* **2021**, *11*, 3782–3790. [CrossRef]
29. Mazen Alhato, M.; Bouallègue, S.; Rezk, H. Modeling and Performance Improvement of Direct Power Control of Doubly-Fed Induction Generator Based Wind Turbine through Second-Order Sliding Mode Control Approach. *Mathematics* **2020**, *8*, 2012. [CrossRef]
30. Nasiri, M.; Mobayen, S.; Zhu, Q.M. Super-twisting sliding mode control for gear less PMSG-based wind turbine. *Complexity* **2019**, *2019*, 1–15. [CrossRef]
31. Venu, G.; Kalyani, S.T. Design of fractional order based super twisting algorithm for BLDC motor. In Proceedings of the 2019 3rd International Conference on Trends in Electronics and Informatics (ICOEI), Tirunelveli, India, 23–25 April 2019; pp. 271–277. [CrossRef]
32. Rakhtala, S.M.; Casavola, A. Real time voltage control based on a cascaded super twisting algorithm structure for DC-DC converters. *IEEE Trans. Ind. Electron.* **2021**, 1. [CrossRef]
33. Sriprang, S.; Nahid-Mobarakeh, B.; Takorabet, N.; Pierfederici, S.; Bizon, N.; Kuman, P.; Thounthong, P. Permanent Magnet Synchronous Motor Dynamic Modeling with State Observer-based Parameter Estimation for AC Servomotor Drive Application. *Appl. Sci. Eng. Prog.* **2019**, *12*, 286–297. [CrossRef]
34. Benbouhenni, H. Intelligent super twisting high order sliding mode controller of dual-rotor wind power systems with direct attack based on doubly-fed induction generators. *J. Electr. Eng. Electron. Control. Comput. Sci.* **2021**, *7*, 1–8. Available online: https://jeeeccs.net/index.php/journal/article/view/219. (accessed on 1 September 2021).
35. Shah, A.P.; Mehta, A.J. Direct power control of grid-connected DFIG using variable gain super-twisting sliding mode controller for wind energy optimization. In Proceedings of the IECON 2017—43rd Annual Conference of the IEEE Industrial Electronics Society, Beijing, China, 5–8 November 2017; pp. 2448–2454. [CrossRef]
36. Kelkoul, B.; Boumediene, A. Stability analysis and study between classical sliding mode control (SMC) and super twisting algorithm (STA) for doubly fed induction generator (DFIG) under wind turbine. *Energy* **2021**, *214*, 118871. [CrossRef]

37. Bouyekni, A.; Taleb, R.; Boudjema, Z.; Kahal, H. A second-order continuous sliding mode based on DFIG for wind-turbine-driven DFIG. *Elektrotehniški Vestn.* **2018**, *85*, 29–36.
38. Boudjema, Z.; Taleb, R.; Djerriri, Y.; Yahdou, A. A novel direct torque control using second order continuous sliding mode of a doubly fed induction generator for a wind energy conversion system. *Turk. J. Electr. Eng. Comput. Sci.* **2017**, *25*, 965–975. [CrossRef]
39. Benbouhenni, H.; Bizon, N. A Synergetic Sliding Mode Controller Applied to Direct Field-Oriented Control of Induction Generator-Based Variable Speed Dual-Rotor Wind Turbines. *Energies* **2021**, *14*, 4437. [CrossRef]
40. Benbouhenni, H.; Bizon, N. Terminal Synergetic Control for Direct Active and Reactive Powers in Asynchronous Generator-Based Dual-Rotor Wind Power Systems. *Electronics* **2021**, *10*, 1880. [CrossRef]
41. Astolfi, D. Wind Turbine Operation Curves Modelling Techniques. *Electronics* **2021**, *10*, 269. [CrossRef]
42. Beik, O.; Al-Adsani, A.S. Active and Passive Control of a Dual Rotor Wind Turbine Generator for DC Grids. *IEEE Access* **2021**, *9*, 1987–1995. [CrossRef]
43. Luo, X.; Niu, S. A Novel Contra-Rotating Power Split Transmission System for Wind Power Generation and Its Dual MPPT Control Strategy. *IEEE Trans. Power Electron.* **2017**, *32*, 6924–6935. [CrossRef]
44. Zhao, Y.; Teng, D.; Li, D.; Zhao, X. Comparative Research on Four-Phase Dual Armature-Winding Wound-Field Doubly Salient Generator with Distributed Field Magnetomotive Forces for High-Reliability Application. *IEEE Access* **2021**, *9*, 12579–12591. [CrossRef]
45. Zhao, W.; Lipo, T.A.; Kwon, B. A Novel Dual-Rotor, Axial Field, Fault-Tolerant Flux-Switching Permanent Magnet Machine with High-Torque Performance. *IEEE Trans. Magn.* **2015**, *51*, 1–4. [CrossRef]
46. Fukami, T.; Momiyama, M.; Shima, K.; Hanaoka, R.; Takata, S. Steady-State Analysis of a Dual-Winding Reluctance Generator with a Multiple-Barrier Rotor. *IEEE Trans. Energy Convers.* **2008**, *23*, 492–498. [CrossRef]
47. Wang, Y.; Niu, S.; Fu, W. A Novel Dual-Rotor Bidirectional Flux-Modulation PM Generator for Stand-Alone DC Power Supply. *IEEE Trans. Ind. Electron.* **2019**, *66*, 818–828. [CrossRef]
48. Yahdou, A.; Djilali, A.B.; Boudjema, Z.; Mehedi, F. Improved vector control of a counter-rotating wind turbine system using adaptive backstepping sliding mode. *J. Eur. Des. Syst. Autom.* **2020**, *53*, 645–651.
49. Anthony, M.; Prasad, V.; Kannadasan, R.; Mekhilef, S.; Alsharif, M.H.; Kim, M.-K.; Jahid, A.; Aly, A.A. Autonomous Fuzzy Controller Design for the Utilization of Hybrid PV-Wind Energy Resources in Demand Side Management Environment. *Electronics* **2021**, *10*, 1618. [CrossRef]
50. Huangfu, Y.; Xu, J.; Zhao, D.; Liu, Y.; Gao, F. A Novel Battery State of Charge Estimation Method Based on a Super-Twisting Sliding Mode Observer. *Energies* **2018**, *11*, 1211. [CrossRef]
51. Ha, L.N.N.T.; Hong, S.K. Robust Dynamic Sliding Mode Control-Based PID–Super Twisting Algorithm and Disturbance Observer for Second-Order Nonlinear Systems: Application to UAVs. *Electronics* **2019**, *8*, 760. [CrossRef]
52. Shi, D.; Wu, Z.; Chou, W. Super-Twisting Extended State Observer and Sliding Mode Controller for Quad rotor UAV Attitude System in Presence of Wind Gust and Actuator Faults. *Electronics* **2018**, *7*, 128. [CrossRef]
53. Listwan, J. Application of super-twisting sliding mode controllers in direct field-oriented control system of six-phase induction motor: Experimental studies. *Power Electron. Drives* **2018**, *3*, 23–34. [CrossRef]
54. Shen, X.; Liu, J.; Marquez, A.; Luo, W.; Leon, J.I.; Vazquez, S.; Franquelo, L.G. A High-Gain Observer-Based Adaptive Super-Twisting Algorithm for DC-Link Voltage Control of NPC Converters. *Energies* **2020**, *13*, 1110. [CrossRef]
55. Chen, S.; Zhang, X.; Wu, X.; Tan, G.; Chen, X. Sensorless Control for IPMSM Based on Adaptive Super-Twisting Sliding-Mode Observer and Improved Phase-Locked Loop. *Energies* **2019**, *12*, 1225. [CrossRef]
56. Uddin, W.; Zeb, K.; Adil Khan, M.; Ishfaq, M.; Khan, I.; Islam, S.U.; Kim, H.-J.; Park, G.S.; Lee, C. Control of Output and Circulating Current of Modular Multilevel Converter Using a Sliding Mode Approach. *Energies* **2019**, *12*, 4084. [CrossRef]
57. Dendouga, A. Conventional and Second Order Sliding Mode Control of Permanent Magnet Synchronous Motor Fed by Direct Matrix Converter: Comparative Study. *Energies* **2020**, *13*, 5093. [CrossRef]
58. Zeb, K.; Busarello, T.D.C.; Ul Islam, S.; Uddin, W.; Raghavendra, K.V.G.; Khan, M.A.; Kim, H.-J. Design of Super Twisting Sliding Mode Controller for a Three-Phase Grid-connected Photovoltaic System under Normal and Abnormal Conditions. *Energies* **2020**, *13*, 3773. [CrossRef]
59. Kafi, M.R.; Hamida, M.A.; Chaoui, H.; Belkacemi, R. Sliding Mode Self-Sensing Control of Synchronous Machine Using Super Twisting Interconnected Observers. *Energies* **2020**, *13*, 4199. [CrossRef]
60. Liu, Y.; Fang, J.; Tan, K.; Huang, B.; He, W. Sliding Mode Observer with Adaptive Parameter Estimation for Sensorless Control of IPMSM. *Energies* **2020**, *13*, 5991. [CrossRef]
61. Valenzuela, F.A.; Ramírez, R.; Martínez, F.; Morfín, O.A.; Castañeda, C.E. Super-Twisting Algorithm Applied to Velocity Control of DC Motor without Mechanical Sensors Dependence. *Energies* **2020**, *13*, 6041. [CrossRef]
62. Azzouz, T.; Abdelhamid, B. Performance of PI controller for control of active and reactive power in DFIG operating in a grid-connected variable speed wind energy conversion system. *Front. Energy* **2014**, *8*, 371–378. [CrossRef]
63. Karima, B.; Akkila, B. Output power control of a variable wind energy conversion system. *Rev. Sci. Tech. Electrotech. Energ.* **2017**, *62*, 197–202.
64. Amrane, F.; Chaiba, A. A novel direct power control for grid-connected doubly fed induction generator based on hybrid artificial intelligent control with space vector modulation. *Rev. Sci. Tech. Electrotech. Energ.* **2016**, *61*, 263–268.

65. Amrane, F.; Chaiba, A.; Badr Eddine, B.; Saad, M. Design and implementation of high performance field oriented control for grid-connected doubly fed induction generator via hysteresis rotor current controller. *Rev. Roum. Rev. Sci. Tech. Electrotech. Energ.* **2016**, *61*, 319–324.
66. Yusoff, N.A.; Razali, A.M.; Karim, K.A.; Sutikno, T.; Jidin, A. A Concept of Virtual-Flux Direct Power Control of Three-Phase AC-DC Converter. *Int. J. Power Electron. Drive Syst.* **2017**, *8*, 1776–1784. [CrossRef]
67. Quan, Y.; Hang, L.; He, Y.; Zhang, Y. Multi-Resonant-Based Sliding Mode Control of DFIG-Based Wind System under Unbalanced and Harmonic Network Conditions. *Appl. Sci.* **2019**, *9*, 1124. [CrossRef]
68. Yahdou, A.; Hemici, B.; Boudjema, Z. Second order sliding mode control of a dual-rotor wind turbine system by employing a matrix converter. *J. Electr. Eng.* **2016**, *16*, 1–11.
69. Yaichi, I.; Semmah, A.; Wira, P.; Djeriri, Y. Super-twisting sliding mode control of a doubly-fed induction generator based on the SVM strategy. *Period. Polytech. Electr. Eng. Comput. Sci.* **2019**, *63*, 178–190. [CrossRef]